A UNIFIED MOBILITY MODEL FOR DEVICE SIMULATION—I. MODEL EQUATIONS AND CONCENTRATION DEPENDENCE

D. B. M. KLAASSEN

Philips Research Laboratories, P.O. Box 80000, 5600 JA Eindhoven, The Netherlands

Abstract—The first physics-based analytical model is presented that unifies the descriptions of majority and minority carrier mobility and that includes screening of the impurities by charge carriers, electron–hole scattering, clustering of impurities and the full temperature dependence of both majority and minority carrier mobility. Using this model, excellent agreement is obtained with published experimental data on Si. The model is especially suited for device simulation purposes, because the carrier mobility is given as an analytical function of the donor, acceptor, electron and hole concentrations and of the temperature.

1. INTRODUCTION

The results of device simulations depend critically on the physical models used, e.g. lifetime, recombination and mobility of carriers, and bandgap narrowing. Sometimes experimental information is only available on a combination of mechanisms, e.g. bandgap narrowing in combination with mobility. With respect to the carrier mobility, however, independent data are also available. During the last few years, a number of experimental results have been published which show that, starting at a doping concentration of 10^{18} cm^{-3}, the minority carrier mobility in Si exceeds the majority carrier mobility, up to a factor of three at a concentration of 10^{20} cm^{-3} (for electrons see Ref. [1]; for holes see Refs [2–6]).

Theoretical calculations have also shown that the minority carrier mobility may exceed the majority carrier mobility at low temperatures[7] or at high doping concentrations[8]. However, they did not result in formulations for the mobility that can be used in device simulation programs. Several analytical fit functions describing the experimental data on the minority carrier mobility as a function of the impurity concentration have been proposed[1,2,3,5]. However, for device simulation programs the mobility should be expressed as a single function of the local donor and acceptor concentrations. Switching between separate functions for minority and majority mobility may result in abrupt changes in mobility and therefore cause numerical problems. This problem is avoided in the mobility model published by Shigyo *et al.*[9]. As their model is based on empirical expressions for majority and minority mobility as functions of donor and acceptor concentration, it is restricted to room temperature and, moreover, electron–hole scattering is not taken into account. For the minority carrier mobility electron–hole scattering

is as important as impurity scattering, because the concentration of unlike carriers equals the impurity concentration.

In the model presented here the main contributions to the mobility are taken into account: besides lattice, donor and acceptor scattering, electron–hole scattering is also incorporated. Screening of impurities by charge carriers and the temperature dependence of both majority and minority carrier mobility are included. The model is carefully constructed to yield a majority carrier mobility that is exactly equal to the empirical expression published by Masetti *et al.*[10], which is widely used in device simulation programs. To obtain this goal this expression is used as a starting point to identify the scattering mechanisms contributing to the majority carrier mobility. Next, theoretically calculated mobility ratios are used to obtain the impurity as well as the electron–hole scattering mobility. Analytical fit functions are presented, which describe the theoretically calculated ratios in fair detail. The large number of computations on which these fit functions are based were only feasible by the use of theoretical approximations (e.g. Boltzmann statistics, JWKB phase shift approximation) that contain all the essential details. Using the analytical (fit) functions, the carrier mobility is given as an analytical function of the donor, acceptor, electron and hole concentrations. Therefore, the resulting model is especially suited for device simulation purposes.

The main features of the model and a limited comparison with experimental data have been published elsewhere[11]. Here the full details and a complete comparison with experimental data on the concentration dependence of the mobility will be presented. A comparison with experimental data on the temperature dependence of the mobility will be published in a companion paper[12].

2. CONTRIBUTIONS TO THE MOBILITY

There are four contributions to the carrier mobility: lattice, donor, acceptor and electron–hole scattering. Electron–electron and hole–hole scattering is not accounted for, as it represents only a second-order effect on the mobility[13]. In this section the four contributions to the mobility mentioned above will be discussed.

2.1. Lattice scattering

Experimental data on the majority electron and hole mobilities as functions of impurity concentration N at 300 K are well described by ([10] and Fig. 1):

$$\mu = \mu_{min} + \frac{\mu_{max} - \mu_{min}}{1 + (N/N_{ref,1})^{\alpha_1}} - \frac{\mu_1}{1 + (N_{ref,2}/N)^{\alpha_2}}. \quad (1)$$

The coefficients in eqn (1) for electrons and holes are given in Table 1 (see also Ref. [10]). Since we want to retain this good description of the majority mobility in our model, we use eqn (1) as a starting point. At very low impurity concentrations the only scattering mechanism is lattice scattering. So the electron mobility due to lattice scattering $\mu_{e,L}$ and the hole mobility due to lattice scattering $\mu_{h,L}$ are the low-concentration limits of eqn (1):

$$\mu_{i,L} = \mu_{max}, \quad (2)$$

where the subscript i stands for e or h, and μ_{max} has to be chosen from Table 1 accordingly.

2.2. Majority impurity scattering including screening

The third term on the right-hand side of eqn (1) is negligible up to doping levels of $10^{20}\,cm^{-3}$ (see Fig. 1). Effects of ultra-high concentrations on the carrier mobility, described by this third term, will be treated in a separate section (Section 3). The remaining two terms in eqn (1) are the familiar Caughey–Thomas expression for the carrier mobility[21]. The electron mobility due to donor scattering $\mu_{e,D}$ and the hole mobility due to acceptor scattering $\mu_{h,A}$ are obtained by subtracting the lattice scattering mobil-
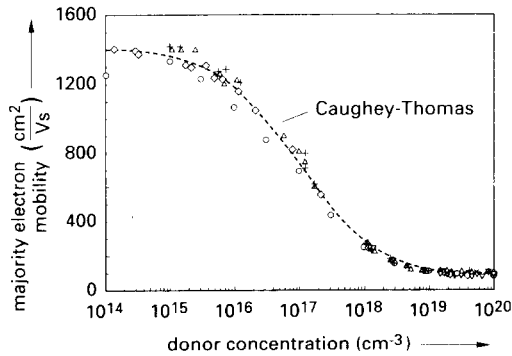

Fig. 1. Majority electron mobility as a function of the donor concentration. Symbols represent literature data: ◯[14]; △[15]; +[16]; ×[17]; ◇[18–20]; and ▽[10]. The dashed line represents the first two terms of eqn (1).

Table 1. Model parameters for the majority electron mobility (As and P) and majority hole mobility (B) given by eqn (1) (see Ref. [10] and Fig. 1)

Parameter	A→As	P	B
μ_{max}(cm^2 V^{-1} s^{-1})	1417.0	1414.0	470.5
μ_{min}(cm^2 V^{-1} s^{-1})	52.2	68.5	44.9
μ_1(cm^2 V^{-1} s^{-1})	43.4	56.1	29.0
$N_{ref,1}$(cm^{-3})	9.68×10^{16}	9.20×10^{16}	2.23×10^{17}
$N_{ref,2}$(cm^{-3})	3.43×10^{20}	3.41×10^{20}	6.10×10^{20}
α_1	0.68	0.711	0.719
α_2	2.0	1.98	2.0

ity, $\mu_{e,L}$ or $\mu_{h,L}$, from eqn (1) using Matthiesen's rule. The resulting expression reads:

$$\mu_{i,I}(N_I) = \mu_{i,N}\left(\frac{N_{ref,1}}{N_I}\right)^{\alpha_1} + \mu_{i,c}, \quad (3a)$$

with

$$\mu_{i,N} = \frac{\mu_{max}^2}{\mu_{max} - \mu_{min}} \quad (3b)$$

and

$$\mu_{i,c} = \frac{\mu_{min}\mu_{max}}{\mu_{max} - \mu_{min}}, \quad (3c)$$

where the subscripts (i, I) stand for (e, D) or (h, A); N_D is the donor and N_A is the acceptor concentration. The parameters μ_{max}, μ_{min}, $N_{ref,1}$ and α_1 have to be chosen from Table 1 accordingly. It should be noted that Matthiesen's rule, which is used to obtain the contribution to the mobility given by eqn (3a), is an approximation in itself. As, however, Matthiesen's rule will again be used to sum all contributions to the mobility in Section 4, possible errors may cancel.

At high carrier concentrations carriers tend to screen impurities from other carriers. Consequently, the Brooks–Herring theory, which starts from a screened Coulomb potential, yields a collison cross-section for impurity scattering that depends only on the carrier concentration c (see e.g.[22]). The collision cross-section for majority impurity scattering $\sigma_{i,I}$ obtained from eqn (3a) reads:

$$\sigma_{i,I} \propto \{N_I\mu_{i,I}\}^{-1}$$
$$= \{\mu_{i,N}(N_{ref,1})^{\alpha_1}(N_I)^{1-\alpha_1} + \mu_{i,c}N_I\}^{-1}. \quad (4)$$

Following the Brooks–Herring theory by simply replacing the impurity concentration N_I by the carrier concentration c in eqn (4), yields an infinite collision cross-section at zero carrier concentration (i.e. weak screening). This problem is solved in the statistical screening theory of Ridley[13,23,24], which merges the Conwell–Weisskopf[24,25] and Brooks–Herring approaches: $\sigma_{i,I}$ is at low concentrations a function of N_I and at high concentrations a function of c. As the second term in eqn (4) is predominant at high concentrations, in our approach only in this term is the impurity concentration N_I replaced by the carrier concentration c. The resulting expression for $\mu_{i,I}$ reads:

$$\mu_{i,I}(N_I, c) = \mu_{i,N}\left(\frac{N_{ref,1}}{N_I}\right)^{\alpha_1} + \mu_{i,c}\left(\frac{c}{N_I}\right). \quad (5)$$

From eqn (5) it can be seen that due to screening at high impurity concentrations the impurity scattering mobility increases with the carrier concentration.

2.3. Minority impurity scattering

Already in a paper published in 1957 Blatt[7] showed that at low temperatures the Born approximation breaks down and that from the superior partial-wave method it can be concluded that "in that energy range majority impurities scatter much more effectively than minority impurities". A similar breakdown of the Born approximation occurs at high carrier concentrations[8]. In the partial-wave method the collision cross-section for linear-momentum relaxation σ_τ can be evaluated from the quantum mechanical phase shifts using eqn (6.29) of Ref. [26]. Using the JWKB approximation for the phase shifts (see eqn (IVb.1c) of Ref. [27]; [28]) we calculated the ratio $G(P)$ between the collision cross-sections for repulsive ($\sigma_{\tau,\text{rep}}$) and attractive ($\sigma_{\tau,\text{attr}}$) screened Coulomb potentials (see Fig. 2):

$$G(P) = \frac{\sigma_{\tau,\text{rep}}}{\sigma_{\tau,\text{attr}}} = \frac{\sigma_{\text{min}}}{\sigma_{\text{maj}}} = \frac{\mu_{\text{maj}}}{\mu_{\text{min}}} \rightarrow \frac{\mu_{e,D}}{\mu_{e,A}} \quad \text{or} \quad \rightarrow \frac{\mu_{h,A}}{\mu_{h,D}}, \quad (6)$$

as a function of

$$P = 4k^2 r_0^2, \quad (7)$$

where k is the wave vector and r_0 is the Debye screening length[13]. In the theoretical calculation of the mobility from the energy-dependent collision cross-section, this parameter P is evaluated at an energy of $3k_B T$, where k_B is Boltzmann's constant and T is the temperature (see p. 267 of Ref. [26]). Consequently, we also evaluated the parameter P given by eqn (7) at this temperature, yielding (with the permittivity of Si):

$$P = \frac{1.36 \times 10^{20}}{c} \left(\frac{m}{m_0}\right)\left(\frac{T}{300}\right)^2, \quad (8)$$

where m is the effective carrier mass, m_0 is the free carrier mass, T is the temperature in kelvin and c is
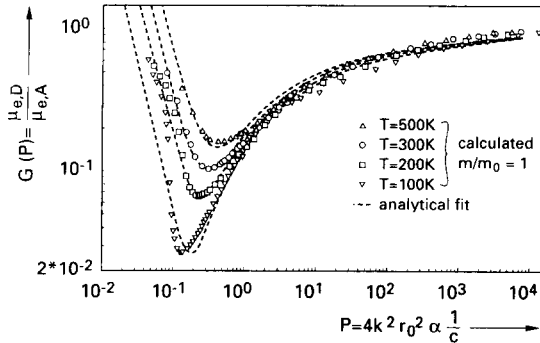

Fig. 2. The ratio $G(P)$ calculated as a function of P [see eqns (6) and (8)] for four different temperatures and an effective carrier mass equal to the free carrier mass. The dashed line represents the analytical fit given by eqn (9).

Table 2. Numerical values for the constants s_i in eqn (9) and r_i in eqn (12)

i	s_i	r_i
1	0.89233	0.7643
2	0.41372	2.2999
3	0.19778	6.5502
4	0.28227	2.3670
5	0.005978	−0.01552
6	1.80618	0.6478
7	0.72169	

the carrier concentration in cm^{-3}. From Ref. [7] it can be seen that at given P the cross-sections are still a function of carrier mass and temperature. From Fig. 2 it can be seen that the ratio $G(P)$ given by eqn (6) for fixed P increases with temperature. Additional calculations were performed for different values of the carrier mass and at the same temperatures as given in Fig. 2. These results showed that the ratio $G(P)$ for fixed P and temperature increases with decreasing carrier mass. All results could be described by an analytical fit formula (see Fig. 2):

$$G(P) = 1 - \frac{s_1}{\left\{s_2 + \left(\frac{m_0}{m}\frac{T}{300}\right)^{s_4} P\right\}^{s_3}}$$

$$+ \frac{s_5}{\left\{\left(\frac{m}{m_0}\frac{300}{T}\right)^{s_7} P\right\}^{s_6}}, \quad (9)$$

where T is the temperature in kelvin. The numerical values of the constants in this formula are given in Table 2. It should be noted that the accuracy of the JWKB approximation for the phase shifts was checked against the results obtained by Blatt (Fig. 6 of Ref. [7]). For all values of P with $G(P) \leqslant 1$ good agreement was obtained. Only at very small values of P did differences occur due to the JWKB approximation.

The contribution to the electron mobility due to acceptor scattering $\mu_{e,A}$ and the contribution to the hole mobility due to donor scattering $\mu_{h,D}$ are now obtained from:

$$\mu_{e,A}(N_A, c) = \frac{\mu_{e,D}(N_D = N_A, c)}{G(P_e)}$$

and

$$\mu_{h,D}(N_D, c) = \frac{\mu_{h,A}(N_A = N_D, c)}{G(P_h)}, \quad (10)$$

where $\mu_{e,D}$ and $\mu_{h,A}$ are given by eqn (5). The subscript e and h of P indicates that the effective electron and hole mass, respectively, has to be used in eqn (8).

2.4. Electron–hole scattering

As far as the attractive interaction potential for electron–hole scattering is concerned, holes can be regarded as moving donors and electrons can be regarded as moving acceptors. The relaxation time

for the linear momentum of the primary scatterer τ in a system of two moving scattering partners is[29]:

$$\frac{1}{\tau} = 2\pi M_2 \int_{v_2=0}^{\infty} \int_{\theta=0}^{\pi} f_2\left(1 - \frac{v_2}{v_1}\cos\theta\right)$$
$$\times g\sigma_\tau v_2^2 \sin\theta \; d\theta \; dv_2. \quad (11)$$

where v_1 is the primary velocity, v_2 is the secondary velocity, θ is the angle between v_1 and v_2, g is the relative velocity, f_2 is taken to be the Boltzmann distribution function normalized to the concentration of secondary scatterers; and $M_2 = m_2/(m_1 + m_2)$, with m_1 and m_2 the mass of the primary and secondary scatterers, respectively. From the relaxation time given by eqn (11) the mobility can be evaluated using standard procedures (see eqn (8.25) and p. 267 of Ref. [26]). The mobility ratio $F(P)$ between stationary secondary scatterers with infinite mass and moving secondary scatterers with finite mass can be calculated accurately using the Brooks–Herring (or Born) approximation, which yields for attractive potentials almost the same collision cross-sections as the partial-wave method (see Fig. 6 of Ref. [7]). At fixed P the $F(P)$ is still a function of the mass ratio but independent of the temperature (see Fig. 3). All results could be described by an analytical fit formula:

$$F(P) = \frac{r_1 P^{r_6} + r_2 + r_3 \dfrac{m_1}{m_2}}{P^{r_6} + r_4 + r_5 \dfrac{m_1}{m_2}}. \quad (12)$$

The numerical values of the constants in this formula are given in Table 2.

The contribution to the electron mobility due to hole scattering $\mu_{e,h}$ and the contribution to the hole mobility due to electron scattering $\mu_{h,e}$ are now obtained using:

$$\mu_{e,h}(p, c) = F(P_e)\mu_{e,D}(N_D = p, c)$$

and

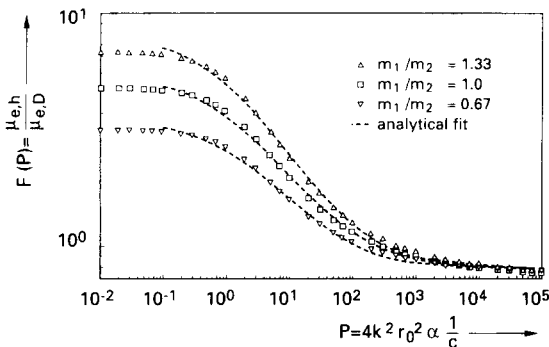$$\mu_{h,e}(n, c) = F(P_h)\mu_{h,A}(N_A = n, c), \quad (13)$$

Fig. 3. The function $F(P)$ calculated as a function of P [see eqns (8)] for three different mass ratios. The dashed line represents the analytical functions given by eqn (12).
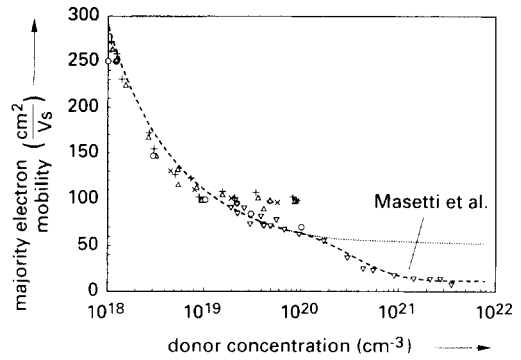

Fig. 4. Majority electron mobility as a function of the donor concentration. Symbols represent literature data: $\bigcirc$[14]; $\triangle$[15]; $+$[16]; $\times$[17]; $\Diamond$[18–20]; and ∇[10]. The dotted line represents the first two terms of eqn (1) and the dashed line represents all three terms of eqn (1).

where $\mu_{e,D}$ and $\mu_{h,A}$ are again given by eqn (5); p is the hole concentration and n is the electron concentration. It should be noted that as $F(P) \leqslant 1/G(P)$, carrier scattering is more important for the minority carrier mobility than impurity scattering.

3. ULTRA-HIGH CONCENTRATION EFFECTS

At ultra-high concentrations the Caughey–Thomas formula no longer suffices to describe the carrier mobility and the full formula of Masetti et al.[10] has to be used [see eqn (1) and Fig. 4]. These effects of ultra-high concentrations on the mobility represented by the third term on the right-hand side of eqn (1), can be accounted for by assuming that above an impurity concentration of 10^{20} cm^{-3} the carriers are no longer scattered by impurities possessing one electronic charge and a concentration N_I, but by impurities with Z electronic charges and a "cluster" concentration $N_I' = N_I/Z$. The concentration of charge carriers c is not affected. In the Appendix it is shown that these ultra-high concentration effects on the carrier mobility can be modelled effectively by replacing N_I by $Z \times N_I$ in eqn (5). This modified majority impurity scattering mobility is added to the lattice scattering mobility using Matthiesen's rule. The resulting mobility is now equated to the full eqn (1). Solving for Z at each impurity concentration N_I yields the "clustering" function $Z_I(N_I)$, which can be described in reasonable detail by the following analytical fit function (see Fig. 5):

$$Z_I(N_I) = 1 + \frac{1}{c_I + \left(\dfrac{N_{\text{ref},I}}{N_I}\right)^2}. \quad (14)$$

The subscript I indicates that these calculations have to be done for each set of parameters given in Table 1. The sets for As and P yielded the same results within a few percent and can be described by $c_D = 0.21$ and $N_{\text{ref},D} = 4.0 \times 10^{20}$ cm^{-3}. For B we found $c_A = 0.50$ and $N_{\text{ref},A} = 7.2 \times 10^{20}$ cm^{-3} (see Fig. 5).
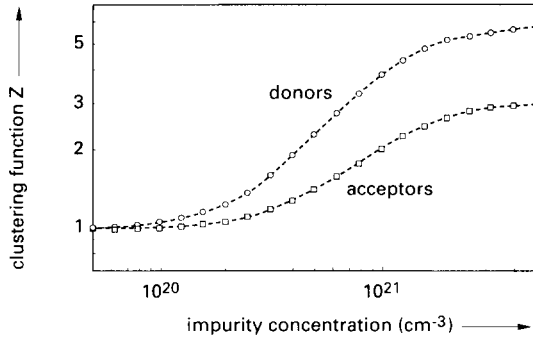
Fig. 5. The clustering functions Z_D (O) and Z_A (□) as a function of N_D and N_A, respectively. The dashed line represents the analytical functions given by eqn (14).

4. MODEL EQUATIONS

We can now obtain the electron mobility μ_e and the hole mobility μ_h as functions of the donor, acceptor, electron and hole concentration.

Starting with ionized donor and acceptor concentrations, $N_{D,s}$ and $N_{A,s}$, the clustering functions have to be applied to calculate the donor and acceptor concentrations N_D and N_A, respectively, to be used in the model [see eqn (14)]:

$$N_D = Z_D(N_{D,s})N_{D,s}$$

and

$$N_A = Z_A(N_{A,s})N_{A,s}. \tag{15}$$

The problem of weak screening $[P \to \infty$ if $c \to 0$, see eqn (8)] is solved by taking for parameter P a weighted harmonic mean of the expression given by eqn (8) for the Brooks–Herring (or Born) approach and its equivalent given by eqn (A3) for the Conwell–Weisskopf approach:

$$P_i(N_I, c) = \left[\frac{f_{CW}}{P_{CW,i}(N_I)} + \frac{f_{BH}}{P_{BH,i}(c)} \right]^{-1}, \tag{16}$$

where the subscript i stands for e or h. If the carrier concentration equals the impurity concentration, P_i will be proportional to $P_{CW,i}$ at low concentrations and to $P_{BH,i}$ at high concentrations (cf. the statistical screening theory of Ridley[13,23,24] and Section 2.2). Note that in eqn (16) the same weighting factors are used for electrons and holes.

Using Matthiesen's rule the total carrier mobility μ_i is now [see eqns (2), (5), (10) and (13)]:

$$\mu_i^{-1} = \mu_{i,L}^{-1} + \mu_{i,D}^{-1} + \mu_{i,A}^{-1} + \mu_{i,j}^{-1}. \tag{17}$$

where $j = $ h if $i = $ e and $j = $ e if $i = $ h. The expression for P_i given by eqn (16) and the last three terms in eqn (17) as given by eqns (5), (10) and (13) have been derived for the situation where there is only one type of scattering partner. In our model we have three types of scattering partners for electrons as well as for holes. In order to ensure that only truly two-body nearest-scatterers are counted among any of the possible scattering partners, in the Conwell–

Weisskopf expression for $P_{CW,i}$ [see eqn (A2)], the impact parameter has to be limited to half the average separation distance of all scattering partners irrespective of the type. Consequently, in the evaluation of eqn (16) instead of N_I:

$$N_{e,sc} = N_D + N_A + p \tag{18a}$$

and

$$N_{h,sc} = N_A + N_D + n, \tag{18b}$$

have to be used. Following the same approach for the collision cross-sections in $\mu_{i,D}$, $\mu_{i,A}$ and $\mu_{i,j}$ [see eqn (A1)], we find for $\mu_{i,D+A+j}$ defined by:

$$\mu_{i,D+A+j}^{-1} = \mu_{i,D}^{-1} + \mu_{i,A}^{-1} + \mu_{i,j}^{-1}, \tag{19}$$

the following expression:

$$\mu_{i,D+A+j}(N_D, N_A, n, p)$$
$$= \mu_{i,N} \frac{N_{i,sc}}{N_{i,sc,eff}} \left(\frac{N_{ref,1}}{N_{i,sc}} \right)^{\alpha_1} + \mu_{i,c} \left(\frac{n+p}{N_{i,sc,eff}} \right), \tag{20}$$

where

$$N_{e,sc,eff} = N_D + G(P_e)N_A + \frac{p}{F(P_e)}, \tag{21a}$$

and

$$N_{h,sc,eff} = N_A + G(P_h)N_D + \frac{n}{F(P_h)}. \tag{21b}$$

An additional advantage of eqns (18–21) is the simplification of the computational procedure.

5. COMPARISON WITH EXPERIMENTAL DATA

In our model developed so far there are four parameters: the electron and hole masses m_e and m_h and the weight factors f_{CW} and f_{BH} in eqn (16). Experimental data are available on the majority mobility, the minority mobility and on the effect of electron–hole scattering[30,31]. We designed the model to yield for the majority mobility exactly the same results as the expression given in eqn (1). Consequently, there is good agreement between model and experimental data (see Figs 1 and 4).

In a simultaneous interpretation of the experimental data on minority electron mobility, minority hole mobility and electron–hole scattering, the optimal set of parameter values was determined. For $m_h/m_e = 1.258$, $f_{CW} = 2.459$, $f_{BH} = 3.828$ and m_e/m_0 ranging from 0.3 to 1.0, about the same agreement between model calculations and experimental data was found. As for the larger m_e values the agreement was slightly better, we obtained $m_e = m_0$ and $m_h = 1.258m_0$. In Figs 6–8 model calculations using these parameters are compared with the available experimental data.

For the electron minority mobility our model gives about the same results as the fit of Swirhun et al.[1] and good agreement with the experimental data is obtained (see Fig. 6). For the hole minority mobility agreement with experimental data and the fit of
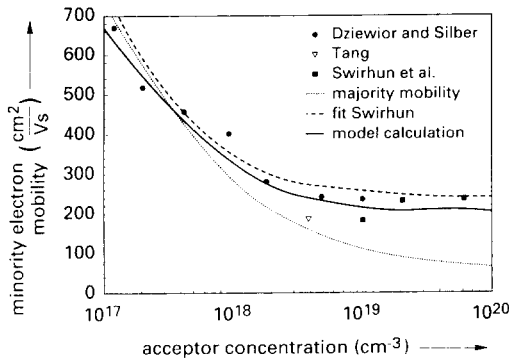
Fig. 6. Minority electron mobility as a function of the acceptor (B) concentration. Symbols represent experimental data: ●[32]; ▽[33]; and ■[1]. The dashed curve represents the fit of Swirhun et al.[1]; the solid curve represents the minority electron mobility using our new model; and the dotted curve represents the majority electron mobility.

del Alamo et al.[2,3] is obtained only at high concentrations. At low concentrations our model yields a minority hole mobility almost equal to the majority hole mobility and smaller than the experimental data of Dziewoir and Silber[32] (see Fig. 7). At this point it is interesting to note that at low concentrations experimental data and our model show a minority electron mobility equal to the majority electron mobility.

Dziewior and Silber found at 10^{17} cm^{-3} a minority hole mobility almost equal to the lattice scattering mobility. Their observations are in disagreement with those of Dannhäuser and Krausse[30,31] who have found that at this concentration electron–hole scattering reduces the mobility by a factor of two (see Fig. 8). Moreover, hole–donor scattering which is not negligible at these concentrations, reduces the minority hole mobility even further. In our physics-based model the effects of minority impurity scattering [function $G(P)$] and electron–hole scattering [function $F(P)$] are linked through the parameter P.
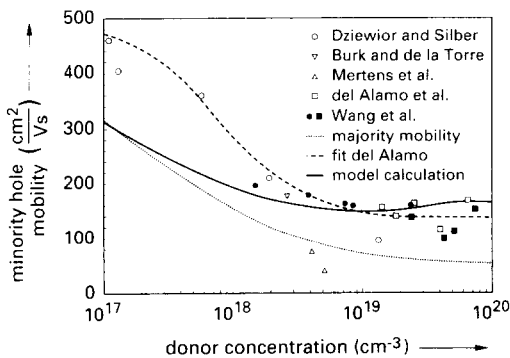

Fig. 7. Minority hole mobility as a function of the donor (P) concentration. Symbols represent experimental data: ○[32]; ▽[34]; △[35]; □[2,3]; ●[5]; and ■[6]. The dashed curve represents the fit of del Alamo et al.[2,3]; the solid curve represents the minority hole mobility using our new model; and the dotted curve represents the majority electron mobility.
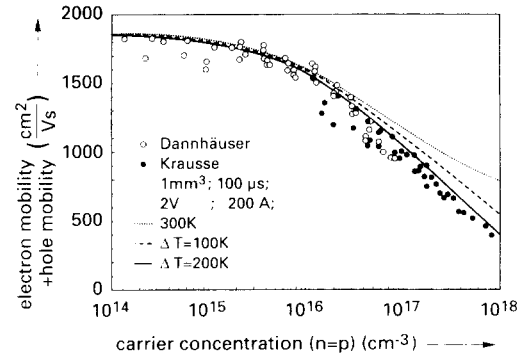

Fig. 8. Sum of electron and hole mobility as a function of carrier concentration. Symbols represent experimental data measured in the intrinsic region of a pin-diode as a function of the injected carrier concentration $(n = p)$: ○[30]; and ●[31]. Curves indicate model calculations: the dotted line represents a temperature of 300 K; the dashed and solid lines represent a temperature increasingly linearly with carrier concentration from 300 K at low concentrations to 400 and 500 K, respectively, at 10^{18} cm^{-3}.

Moreover, effects for minority electrons are related to those for minority holes by the effective masses occurring in the expression for the function $F(P)$. Consequently, varying the parameters in our model does not result in simple independent curve-fitting of the data in Figs 6–8. Using the parameters obtained in the simultaneous interpretation of all the experimental data our model yields results which, in the discrepancy between the results of Dannhäuser and Krausse and those of Dziewior and Silber, tend to favour the former.

At low concentrations, good agreement between our model and the experiments of Dannhäuser and Krausse is obtained, while using room temperature our model yields deviations at high concentrations. At these high concentrations in the experiments of Krausse[31] quite a large power (400 W) is dissipated in a rather small volume (1 mm^3). In spite of the short pulse widths used (100 μs), computer simulations showed that a temperature increase of more than 150 K is quite realistic. With this temperature increase[12] our model also agrees at high concentrations with the data of Dannhäuser and Krausse.

6. CONCLUSIONS

The first physics-based analytical model is presented that unifies the descriptions of majority and minority carrier mobility and that includes screening of the impurities by charge carriers, electron–hole scattering and clustering of impurities. The model is especially suited for device simulation purposes, because the electron and hole mobility are given as analytical functions of local variables: ionized donor, ionized acceptor, electron and hole concentrations. The excellent agreement between our model and published experimental data on the carrier mobility in Si ensures that our model is a sound basis for a revised determination of the bandgap narrowing[36]

and for an extension to less thoroughly investigated aspects of the mobility, e.g. the temperature dependence of the minority carrier mobility[12].

REFERENCES

1. S. E. Swirhun, Y.-H. Kwark and R. M. Swanson, *IEDM Tech. Dig.*, p. 24 (1986).
2. J. del Alamo, S. Swirhun and R. M. Swanson, *IEDM Tech. Dig.*, p. 290 (1985).
3. S. E. Swirhun, J. A. del Alamo and R. M. Swanson, *IEEE Electron Device Lett.* **7**, 168 (1986).
4. J. A. del Alamo and R. M. Swanson, *IEEE Trans. Electron Devices* **ED-34**, 1590 (1987).
5. C. H. Wang, K. Misiakos and A. Neugroschel, *IEEE Trans. Electron Devices* **ED-37**, 1314 (1990).
6. C. H. Wang and A. Neugroschel, *IEEE Electron Device Lett.* **EDL-11**, 576 (1990).
7. F. J. Blatt, *J. Phys. Chem. Solids* **1**, 262 (1957).
8. H. B. Bennett, *Solid-St. Electron.* **26**, 1157 (1983).
9. N. Shigyo, H. Tanimoto, M. Norishima and S. Yasuda, *Solid-St. Electron.* **33**, 727 (1990).
10. G. D. Masetti, M. Severi and S. Solmi, *IEEE Trans. Electron Devices* **ED-30**, 764 (1983).
11. D. B. M. Klaassen, *IEDM Tech. Dig.*, p. 357 (1990).
12. D. B. M. Klaassen, *Solid-St. Electron.* **35**, 961 (1992).
13. B. K. Ridley, *Quantum Process in Semiconductors*, Clarendon Press, Oxford (1988).
14. J. C. Irving, *Bell System Tech. J.* **41**, 387 (1962).
15. F. Mousty, P. Ostoja and L. Passari, *J. Appl. Phys.* **45**, 4576 (1974).
16. G. Baccarani and P. Ostoja, *Solid-St. Electron.* **18**, 579 (1975).
17. M. Finetti and A. M. Mazzone, *J. Appl. Phys.* **48**, 4597 (1977).
18. M. G. Buehler and W. R. Thurber, *IEEE Trans. Electron Devices* **ED-23**, 968 (1976).
19. S. S. Li and W. R. Thurber, *Solid-St. Electron.* **20**, 609 (1977).
20. S. S. Li, In *National Bureau of Standards, Special Publication 400-33*. Washington, DC (1977).
21. D. M. Caughey and R. E. Thomas, *Proc. IEEE.* **55**, 2192 (1967).
22. H. Brooks, *Adv. Electron. Electron Phys.* **7**, 85 (1955).
23. B. K. Ridley, *J. Phys. A* **10**, L79 (1977).
24. B. K. Ridley, *J. Phys. A* **10**, 1589 (1977).
25. E. Conwell and V. F. Weisskopf, *Phys. Rev.* **77**, 388 (1950).
26. F. J. Blatt, *Physics of Electronic Conduction in Solids.* McGraw-Hill, New York (1968).
27. R. B. Bernstein, *Adv. Chem. Phys.* **10**, 75 (1966).
28. A. Messiah, *Quantum Mechanics.* Wiley, New York (1962).
29. S. Chapman and T. G. Cowling, *The Mathematical Theory of Non-uniform Gases.* Cambridge University Press, London (1970).
30. F. Dannhäuser, *Solid-St. Electron.* **15**, 1371 (1972).
31. J. Krausse, *Solid-St. Electron.* **15**, 1377 (1972).
32. J. Dziewior and D. Silber, *Appl. Phys. Lett.* **35**, 170 (1979).
33. D. D. Tang, F. F. Fang, M. Scheuermann, T. C. Chen and G. Sai-Halasz, *IEDM Tech. Dig.*, p. 20 (1986).
34. D. E. Burk and V. de la Torre, *IEEE Electron Device Lett.* **EDL-5**, 231 (1984).
35. R. P. Mertens, J. L. van Meerbergen, J. F. de Nijs and R. J. van Overstraeten, *IEEE Trans. Electron Devices* **ED-27**, 949 (1980).
36. D. B. M. Klaassen, J. W. Slotboom and H. C. de Graaff, *Solid-St. Electron.* **35**, 125 (1992).

APPENDIX

In this Appendix the expression for the majority impurity scattering mobility given by eqn (5) is modified to account for the clustering of impurities possessing one electronic charge and concentration N_I into clusters with Z electronic charges and a concentration $N'_I = N_I/Z$.

The collision cross-section for majority impurity scattering modified to account for screening reads [see eqns (4) and (5)]:

$$\sigma_{i,I} \propto \{N_I \mu_{i,I}\}^{-1} = \{\mu_{i,N}(N_{\text{ref},1})^{z_1}(N_I)^{1-z_1} + \mu_{i,c}c\}^{-1}. \quad (A1)$$

The second term stems via the statistical screening theory of Ridley[13,23,24] from the Brooks–Herring (or Born) approach. In this formulation the collision cross-section is a function of the parameter P_{BH} given by eqn (8):

$$P_{\text{BH}} = \frac{1.36 \times 10^{20}}{c}\left(\frac{m}{m_0}\right)\left(\frac{T}{300}\right)^2, \quad (8)$$

which is independent of the charge on the impurity (see e.g. [13]). The first term in eqn (A1) stems via the statistical screening theory of Ridley from the Conwell–Weisskopf approximation. In this formulation the collision cross-section is a function of the parameter P_{CW} given by (see e.g. [13]):

$$P_{\text{CW}} = \left(\frac{8\pi\epsilon E}{Ze^2}\right)^2 b_{\max}^2 = \left(\frac{4\pi\epsilon E}{Ze^2 N_I^{1/3}}\right)^2, \quad (A2)$$

where ϵ is the permittivity, E is the energy of the charge carrier, e is the electronic charge, Ze is the charge on the impurity and $b_{\max}$ is the maximum impact parameter. The impact parameter is the distance between the impurity and the initial line of motion of the carrier. In the Conwell–Weisskopf approximation this impact parameter is limited to half the average separation distance of the impurities ($b_{\max} = N_I^{-1/3}/2$). Evaluating P_{CW} at $E = 3k_{\text{B}}T$ [as P_{BH}; see eqn (8)], one obtains for Si:

$$P_{\text{CW}} = 3.97 \times 10^{13}\left\{\frac{1}{Z^3 N_I}\left(\frac{T}{300}\right)^3\right\}^{2/3}, \quad (A3)$$

where T is the temperature in kelvin and N_I is the impurity concentration in cm^{-3}. From e.g. [13], it can be seen that in both the Brooks–Herring and the Conwell–Weisskopf approaches the collision cross-section is proportional to Z^2. This leads to the following expression for $\sigma_{i,I}$ modified for impurities with charges larger than one electron charge:

$$\sigma_{i,I} \propto \{N_I \mu_{i,I}\}^{-1} = Z^2 \Big\{ \mu_{i,N}(N_{\text{ref},1})^{z_1}$$

$$\times \left(\frac{300}{T}\right)^{3-3z_1}(Z^3 N_I)^{1-z_1} + \mu_{i,c}\left(\frac{300}{T}\right)^2 c \Big\}^{-1}. \quad (A4)$$

In eqn (A4) we have also accounted for the temperature dependence of the parameters P. In converting the collision cross-section given by eqn (A4) back to the mobility one should note that the energy-dependent prefactor in the relaxation time ($E^{3/2}$ for both BH and CW; see Ref. [13]) yields a temperature-dependent prefactor in the mobility of $T^{3/2}$ (see p. 267 of Ref. [26]). Taking this into account, one finds for the mobility $\mu_{i,I}$:

$$\mu_{i,I}(N_I, c) = Z^{1-z_1}\mu_{i,N}\left(\frac{T}{300}\right)^{3z_1-1.5}\left(\frac{N_{\text{ref},1}}{Z^2 N_I}\right)^{z_1}$$

$$+ \mu_{i,c}\left(\frac{300}{T}\right)^{0.5}\left(\frac{c}{Z^2 N_I}\right). \quad (A5)$$

At high concentrations where the third term on the right-hand side of eqn (1) becomes important, the second term on the right-hand side of eqn (A5) is predominant. In the calculations to obtain Z (see Section 3) the approximation $Z^{1-z_1} \cong 1$ could be made without loss of accuracy. Substituting the cluster concentration N_I/Z for N_I in eqn (A5) now yields a mobility depending on $Z \times N_I$.